Mole-Fraction Imaging of Transverse Injection in a Ducted Supersonic Flow

John D. Abbitt III,* Roy J. Hartfield,* and James C. McDaniel†
University of Virginia, Charlottesville, Virginia 22903

An experimental study has been performed of the mixing characteristics of air injected transversely as underexpanded jets behind a rearward-facing step into a ducted supersonic (Mach 2) air freestream. Laser-induced iodine fluorescence was used to generate two-dimensional images that are processed digitally by laboratory computer in order to yield time-averaged planar injectant mole-fraction distributions. The resulting planar images represent a three-dimensional data base of the time-averaged injectant mole-fraction distribution throughout the flowfield. This data base is used to reconstruct images showing mole-fraction distributions normal to the duct. These images normal to the duct provide a direct representation of the evolution of the supersonic mixing along the duct and allow one-dimensional mixing schedules to be developed from the three-dimensional data base.

Introduction

AIR-breathing engines utilizing supersonic combustion are currently under active development for the propulsion of future hypersonic vehicles. Extensive modeling of supersonic mixing and combustion flowfields has been carried out by a number of investigators in order to optimize combustor design.[1-8] In addition to the theoretical modeling of these flowfields, experiments have been performed to characterize flow patterns and to establish the validity of the computational models.[9,10] Combustion is frequently limited by fuel mixing; therefore, an important aspect of these studies has been the nonreactive mixing.[11-20]

Much of the experimental work on supersonic mixing and combustion has involved the measurement of flowfield properties at pointwise locations using traditional techniques such as gas chromatography and pressure surveys (see, for example, Refs. 11 and 12). Practically, only a relatively small number of points in the flow could be studied with these techniques. Furthermore, the flowfield under consideration becomes altered by the presence of the intrusive collection probes. Flowfield-visualization studies, using the schlieren optical technique,[21] for example, are nonintrusive, but lack the desired spatial resolution in these flowfields.

The present study overcomes these limitations by determining injectant mole-fraction distributions optically and with high spatial resolution in three dimensions. Two-dimensional images are recorded using a digital array camera and planar laser-induced fluorescence from iodine seeded into the injectant airstream. These images are converted into quantitative planar mole-fraction distributions using a recently developed technique.[22] Once multiple planar mole-fraction distributions are obtained, representation of the injectant mole fraction in any desired plane in the flowfield can be easily reconstructed.

The principal objective of this study is to characterize experimentally the injectant mixing patterns that result from air injected sonically and transversely downstream of a rearward-facing step into a Mach 2 airstream. This particular geometry has been studied extensively, both computationally and experimentally. The results reported herein provide a large data base of quantitative injectant mole-fraction measurements for the future validation of computational models of this flowfield.

Experiment

The flowfield used in this study is shown in Fig. 1. A continuous, shock-free Mach 2.07 freestream flow, provided by a two-dimensional Laval nozzle, is introduced into a rectangular duct. Upon entering the duct, the flowfield accelerates and turns past a rearward-facing step through a Prandtl-Meyer expansion fan. The duct entrance is 1.14 cm wide and 0.71 cm high. Two 0.78-mm-diam sonic transverse injectors are located along the duct axial centerline at 3.75 mm and 8.75 mm (three step heights and seven step heights, respectively) downstream of the 1.25-mm rearward-facing step. Both the jets and the tunnel main flow are operated with a stagnation pressure of 202.7 kPa (2 atm) and a temperature of 300 K. Three of the duct walls are made of fused silica in order to provide the necessary optical access.

Iodine is seeded into the air in a mixing chamber located upstream of the tunnel test section. Seeded air can be selected for either the jets or the main flow, or both simultaneously. The maximum change in the air molecular weight due to the iodine seeding is 0.23%, assuming stauration of the air with iodine in the mixing vessel at a seeding fraction of 200 ppm (parts per million). This gives a maximum change in the gas specific heat ratio of 0.01% (due to the iodine vibrational

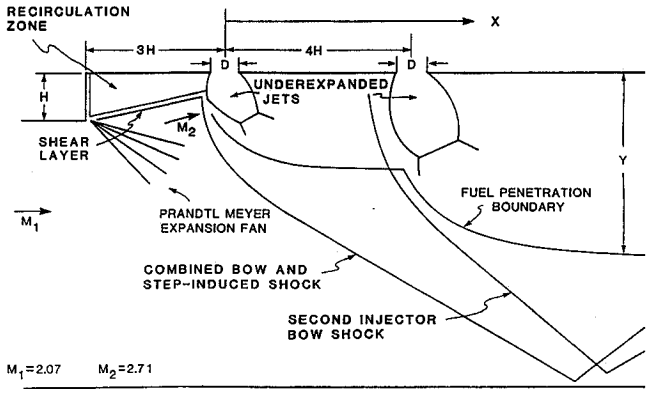

Fig. 1 Flowfield schematic.

Presented as Paper 89-2550 at the AIAA/SAE/ASME/ASEE 25th Joint Propulsion Conference, Monterey, CA, July 1989; received Aug. 16, 1989; revision received Jan. 4, 1990.

*Research Assistant, Aerospace Research Laboratory, Department of Mechanical and Aerospace Engineering.

†Associate Professor, Aerospace Research Laboratory, Department of Mechanical and Aerospace Engineering.

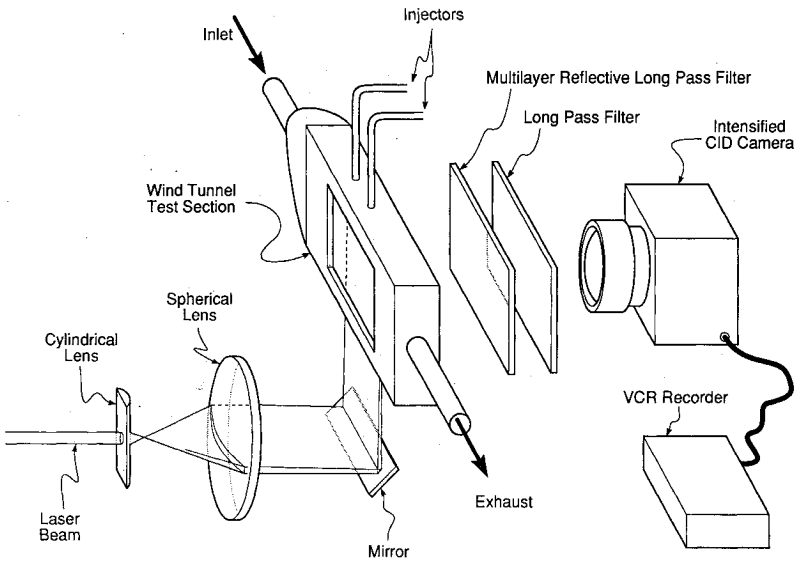

Fig. 2 Experimental apparatus.

population distribution at 300 K) and in the mixture sound speed of −0.11%. Therefore, changes in the thermodynamic properties of the air as a result of the introduction of this level of iodine seeding are negligible. The tracking fidelity of the iodine molecules in air has been shown to be excellent, even across a normal shock wave at a Mach number of 4.[10]

The optical setup used in this study is shown in Fig. 2. Fluorescence from the iodine is induced by a 6-W, argon-ion laser (Spectra Physics Model 171), whose beam is focused, first through a cylindrical lens and then through a spherical lens, to form a 4 cm wide, 100-μm-thick sheet of light. This sheet is positioned in the duct using a micrometer-driven translation stage. The laser is operated at 514.5 nm to excite the overlapping P13, R15 rotational transitions of the (0,43) vibrational band in iodine.

The iodine fluorescence is imaged with a 50-mm focal length, F/2.8 lens onto an intensified charge injection device (CID) array camera (Xybion ISG-207-MUD), after passing through a 560-nm long pass multilayer reflective filter, and a 540-nm long pass absorbing filter. The exposure time for each image is 16.7 ms. The images are recorded using a video cassette recorder (Panasonic AG-6300) in conjunction with a frame indexer (FOR-A VTG-55B) and then digitized using an image capture card (Xybion ImCap-01) installed in a laboratory microcomputer (Standard 286).

Injectant mole-fraciton imaging was performed using a technique recently reported by Hartfield et al.[22] By dividing an image recorded with only the injectant jets seeded with iodine by one recorded with the entire flowfield seeded, the following relation results at each camera picture element (pixel), and corresponding flowfield location:

$$\frac{N_{\mathrm{JET}}}{N_{\mathrm{TOTAL}}} = C\frac{S_{\mathrm{JET}}}{S_{\mathrm{TOTAL}}}$$

In this equation, N_{JET} and N_{TOTAL} are the injectant and total flow number densities, and S_{JET} and S_{TOTAL} are the fluorescence signals recorded by the camera pixel under the two seeding conditions. The C is a constant that is slightly different from unity due to a change in the iodine seeding fraction for the two conditions. (The evaluation of C will be discussed later.)

A value for the intensity of S_{JET} and S_{TOTAL} at each pixel is obtained during the image-digitization process. Each pixel signal level in the image is stored in a file and the intensity is represented by an integer ranging in value from 0–255. The gain of the camera is adjusted so that the full dynamic range of the image-processing equipment could be utilized (i.e., the gain was set so that the relative signal intensity at the pixel which has the maximum value in the image is slightly less than 255). To remove a low-level random noise due to the intensifier and the uncooled CID array, eight images were obtained for each seeding condition and averaged. This reduced the value of the random noise to a level that was below the sensitivity of the camera for the particular gain setting. To eliminate residual elastic scattering from the tunnel surfaces that was not blocked by the optical filters, images were obtained of the laser sheet with the iodine seeding turned off. These background images were subtracted from the images with the seeding present. Four hundred and eighty raw images were required for the total data set which required approximately 2 h to collect. During this time, the stagnation pressure in the tunnel varied less than 1%. The steadiness of the flowfield and the constancy of the stagnation conditions permitted the use of this time-averaged measurement technique. The ratio S_{JET}:S_{TOTAL} at each spatial location was obtained by dividing the values at each pixel in the averaged and background-subtracted images with the jets seeded and with the entire flow seeded. The value of C was determined by utilizing the fact that the injectant mole fraction in the jet core is unity. An average value of the pixels in this core region was measured and the constant C was determined (255, the maximum value, divided by the measured jet core average pixel value). The images were all scaled by the constant C so that regions of 100% injectant mole fraction in all images had a pixel value of 255. The result is a two-dimensional image of the flowfield cross section which shows the time-averaged injectant mole-fraction distribution and can be delineated by either color bands or gray levels. Approximately 38,000 data points, each representing a cross-sectional area of the flowfield of approximately 0.005 mm^2, are resolved in each image in the work reported herein.

Twenty images of the injectant mole fraction were obtained in planes oriented perpendicular to the wall containing the injectors. Imaging began at the tunnel centerline and ended at the outer plane where no fluorescence could be detected. To provide adequate spatial resolution in the flowfield, the spacing between images was 100 μm, approximately one laser sheet thickness. Symmetry of the flow about the tunnel centerline was confirmed and only images in one direction from the tunnel centerline were collected.

The determination of the image scaling constant C is complicated for the images collected off centerline where no jet core region exists. It was, therefore, necessary to establish a

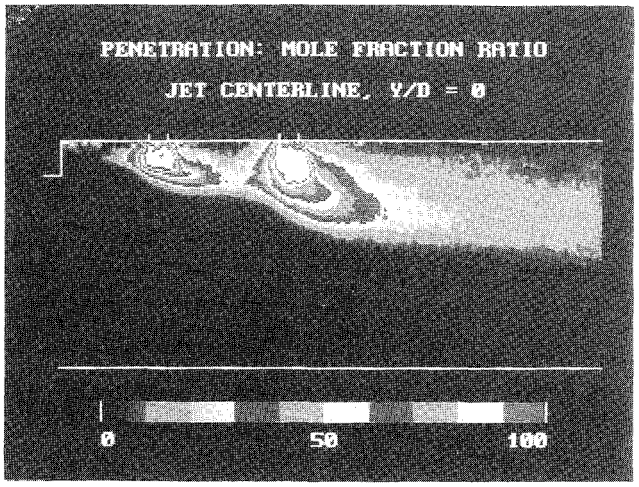

a)

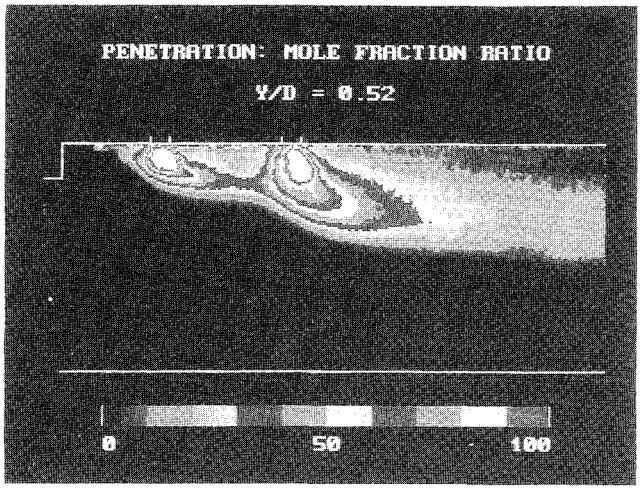

b)

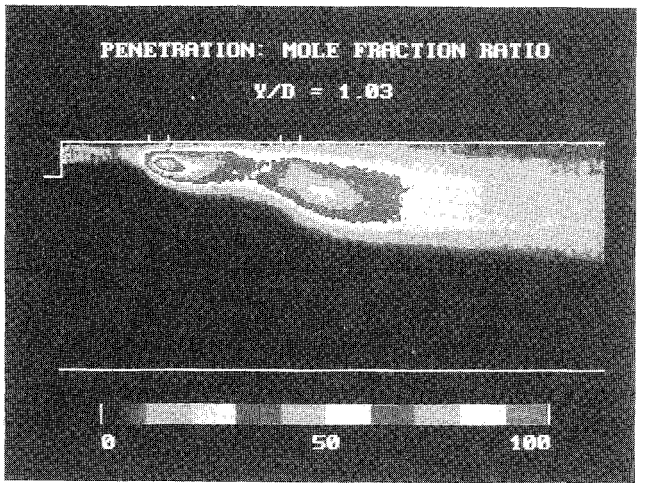

c)

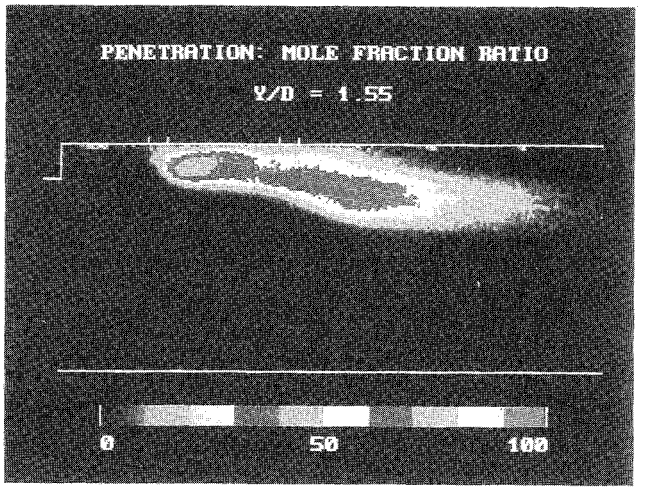

d)

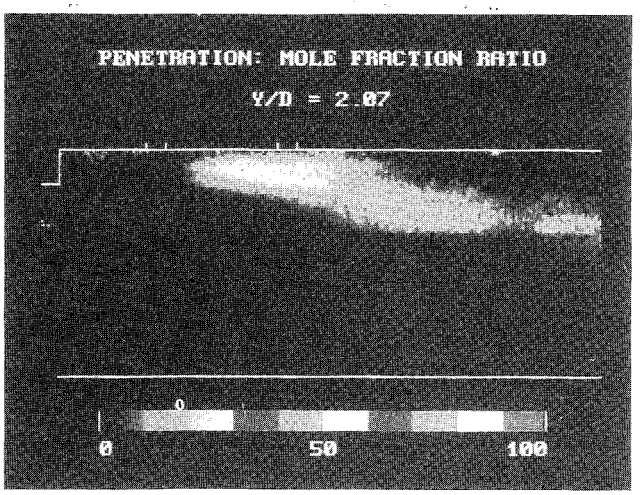

e)

Fig. 3 Mole-fraction distributions.

reference image to which all other images could be scaled. The image along the tunnel centerline was chosen as this reference image. The wind tunnel was then rotated 90 deg and an image of the injectant mole fraction was obtained in a plane oriented parallel to the wall containing the injectors. This rotated image intersected all of the other images. A scaling factor for this rotated image was determined by ensuring that the sum of the pixel values along the line of intersection of this rotated image and the centerline reference image was the same. This rotated image then provided a second method for scaling the off-centerline images. All images that lay outside of the jet core regions were scaled so that the sums of the pixel values along the line common to each off-centerline image and the rotated image were the same. This rotated image was also used as an additional verification of flowfield symmetry.

Results and Discussion

Five of these 20 injectant mole-fraction images are shown in Fig. 3. In these images, injectant mole-fraction contours are shown as bands of varying gray level. Each gray band spans 10% of the mole-fraction distribution. Color images, as well as the actual numerical data files, are also available (contact author) for computational fluid dynamics (CFD) validation purposes. It is important to keep in mind when viewing these images that sharp discontinuities exist between the bands of gray while the change in mole fraction when going from one band to the next is approximately 0.4%. This method of representing the data gives the edges of the contour bands a very jagged appearance. Figure 3a shows the penetration of the injectant along the jet axial centerline. The tunnel walls and the step have been outlined in the image. Markers have also been added to the image to show the location and diameter of the injectors. In this image, the core of the jets where the injectant mole fraction is 100% is apparent. Mixing begins outside the jet core and extends to about 1 jet diameter upstream of the first jet centerline and within 1 jet diameter of the upper wall. Although some mixing does occur in the recirculation region behind the step, the limited dynamic range of the camera does not allow quantitative measurements to be obtained in that re-

gion. Downstream of the first jet, mixing occurs very rapidly, achieving a mole-fraction ratio of 0.3 (stoichiometric value for hydrogen in air) within 3 jet diameters downstream of the first jet and penetrating to about 3 jet diameters from the upper wall. Downstream of the second jet, mixing to a stoichiometric mole fraction of 0.3 is achieved at approximately 4 jet diameters, with penetration to a maximum of about 6 jet diameters. In this centerline plane, little mixing occurs in the vicinity of the wall. This image shows quite clearly that the penetration from the second jet is much greater than that from the first.

In Fig. 3b, a plane located at $Y/D = 0.52$ (0.52 jet diameters from the tunnel centerline) is shown. The core of the jet is still visible in this image. Mixing contours occur slightly further downstream than in Fig. 3a, although penetration is nearly identical. Figure 3c shows a plane located at $Y/D = 1.03$. There is no longer any region of 100% injectant mole fraction in this image. The highest injectant mole-fraction contour is 80% and is in the vicinity of the first jet. Mixing is achieved at approximately the same downstream location as in the previous two images, but covers a larger area, with more mixing close to the wall. It can be seen in Fig. 3d that, at a plane located at $Y/D = 1.55$, the maximum injectant mole fraction is in the 40% range and is located 2 jet diameters downstream of the first jet. It is also seen in this figure that the lateral spreading of injectant from the first jet is greater than that from the second. In Fig. 3e, located at $Y/D = 2.07$, the maximum concentration is found in the 20–30% band as the outer edge of the jet plume is approached.

The 20 planar images, five of which were shown in Fig. 3, represent a quantitative three-dimensional data base of mole-fraction distribution in this supersonic mixing flowfield. This data base can now be used to reconstruct the mixing contours in any desired cross-sectional plane through the flowfield. Figure 4 illustrates mole-fraction distributions in 14 planes reconstructed normal to the duct. Images in this direction would be difficult to collect directly; however, by using the computer to replot the data in this direction, many important features of the mixing are revealed.

The white region in the core of the first jet at X/D of 0 and in the second jet core at X/D of 6 and 7 represent areas where no mixing has occurred. The flow pattern downstream of the jets assumes a distinctive horseshoe shape, which is completely lifted from the wall by an X/D of 10. Splitting, or bifurcation, of the jet plane is seen to occur by X/D of 12. The horseshoe shape and the lifting and bifurcation of the jet plume is due to the strong streamwise vortices that are generated as the jets interact with the supersonic stream. With the experimental capability demonstrated in this paper, one can observe for the first

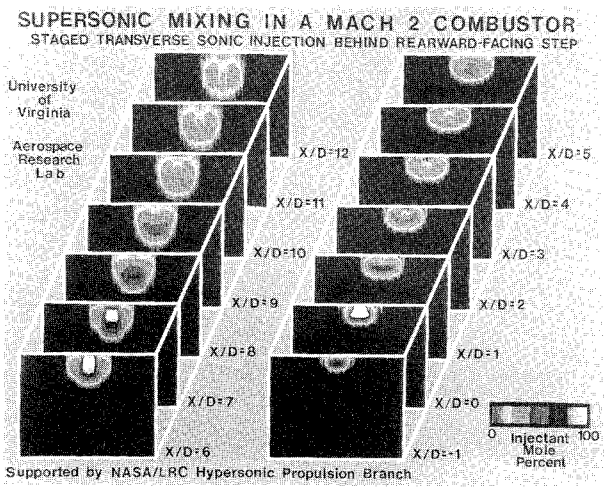

Fig. 4 Mole-fraction distributions in cross-sectional planes.

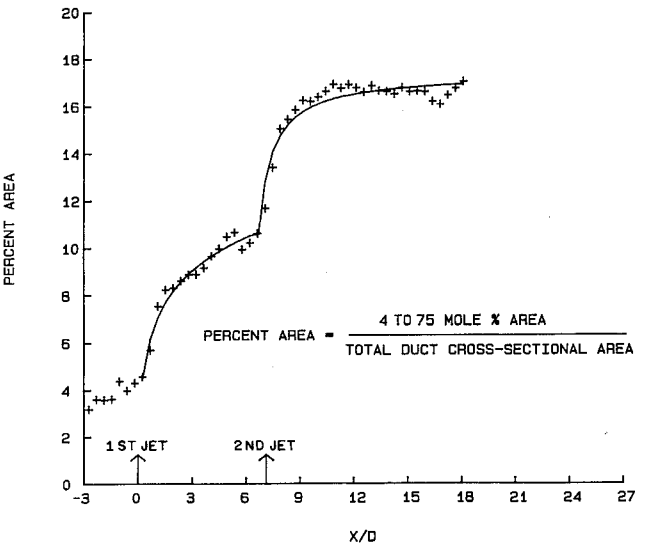

Fig. 5 One-dimensional mixing schedule for transverse staged injection behind a rearward-facing step.

time the strong effect of streamwise vorticity in supersonic mixing flowfields.

As a final step in this study, a "one-dimensional mixing schedule" was developed for use in engine performance codes. The assignment of a number to the degree of mixing at each X/D station is somewhat arbitrary, depending on the mixing definition chosen. However, to illustrate how this data can be used to generate mixing schedules for this flowfield, the degree of mixing at each X/D station was defined as the total area contained between the 4% and 75% mole-fraction contours in that plane, divided by the total cross-sectional area of the duct. This mole-fraction range corresponds to the static flammability limits for hydrogen and air at standard conditions, and certainly contains the region of the flow that is mixed sufficiently to support combustion. Other, perhaps more meaningful, mixing definitions can be used to construct such one-dimensional mixing schedules in the supersonic flowfield. This definition is used only to illustrate the capability to generate easily such mixing schedules once the data is available.

Figure 5 shows the one-dimensional mixing schedule resulting from this mixing definition and developed by having the computer count the number of pixels in each reconstructed cross-sectional image between the 4% and 75% mole-fraction contours and then divide by the total number of pixels in the duct cross section. The resulting percent area is plotted vs X/D as the discrete data points in Fig. 5. A curve fitting to this data is also shown in the figure, with the functions used and the values of the best fit constants given in Table 1. This curve fitting is in a form that can easily be used as a one-dimensional mixing schedule in an engine performance code using this injection geometry. The shape of the mixing schedule illustrates the rapid mixing in the vicinity of the jets and asymptotic approach to a mixed percent area of about 17% by an X/D of about 10. Curves such as the one in Fig. 5 allow an engine de-

Table 1 Parametric equations for one-dimensional mixing schedule

$f(x)$ = percent area

$0.8 < X/D < 6.6$:

$$f(x) = A1 \times \{\ln [A2 \times (X/D + A3)]\} + A4$$

$6.6 < X/D$:

$$f(x) = \{[(X/D - B1) \times B2] / [(X/D - B1) + 1]\} + B3$$

A1 = 2.0912	B1 = 6.8690
A2 = 3.4997	B2 = 5.3219
A3 = 0.1000	B3 = 12.0866
A4 = 4.0629	

signer to evaluate the combustor length required to achieve a desired degree of mixing. (Additional length will, of course, be required for operation at low Damköhler numbers.[23]) Figure 5 also allows one to address the spacing of such injectors needed to fuel the duct to a desired overall fuel equivalence ratio. For the geometry and the mixing definition in this work area, five such injector pairs would fuel the entire duct.

Concluding Remarks

The results of this experiment provide a visual mapping with excellent spatial resolution of the time-averaged mole-fraction distribution of injectant into a supersonic duct. These mole-fraction results measure the true molecular mixing, the quantity of interest in combustion applications. A unique feature of this technique is that since the data are stored in digital form, it is possible to reconstruct a complete two-dimensional image in any desired plane, thus greatly enhancing the ability to study the supersonic mixing phenomena.

With the injection geometry of this study, it was found that mixing is essentially complete by 10 jet diameters downstream from the first jet, with about 17% of the duct cross-sectional area fueled to the static flammability limits. These results are of great interest to the designer of a supersonic combustor. However, the applications of the technique are much broader than supersonic combustion engines and include virtually any situation in which two gas streams are mixed without chemical reaction, whether supersonic or subsonic.

In this experiment, the dynamic range of the data is limited to approximately 100 due to the 8-bit resolution of the digitizer and camera intensifier and to the noise and saturation levels on the camera array. This causes large percentage uncertainties in the mole-fraction contours below 10%. A new unintensified camera with a CCD array, liquid nitrogen cooled for low noise, is being acquired for future studies. This improved camera will permit use of a 14-bit digitizer and will increase the dynamic range of the measurements by about two orders of magnitude, providing much more accuracy in the mole-fraction contours below 10%. This camera will also permit planar determination of the time-averaged velocity field, a measurement that is needed to "see" the vortex structures that are of fundamental importance to supersonic mixing. Extensions of this technique to time-resolved measurements of supersonic mixing and to mixing with combustion are also underway.

From this study, and others at our laboratory and elsewhere,[24] we conclude that efficient mixing in supersonic flow is achieved predominantly through the generation of streamwise vorticity. Any schemes to improve mixing efficiency must recognize this dominant mixing mechanism and focus on the enhancement of the strength of these large-scale, essentially inviscid, vortices and not only the fine-scale turbulence, which is only the final stage of the mixing process.

Acknowledgment

This work was sponsored by NASA Langley Research Center Grants NGT-50142 and NAG-1-795 with G. Burton Northam as technical monitor.

References

[1]Rogers, R. C., "A Study of the Mixing of Hydrogen Injected Normal to a Supersonic Airstream," NASA TN D-6114, March 1971.

[2]Schetz, J. A., and Billig, F. S., "Penetration of Gaseous Jets Injected into a Supersonic Stream," *Journal of Spacecraft,* Vol. 3, Nov. 1966, pp. 1658–1664.

[3]Pan, Y. S., Drummond, J. P., and McClinton, C. R., "Comparison of Two Computer Programs by Predicting Turbulent Mixing of Helium in a Ducted Supersonic Airstream," NASA TP-1166, May 1978.

[4]Drummond, J. P., "Numerical Investigation of the Perpendicular Injector Flowfield in a Hydrogen-Fueled Scramjet," AIAA Paper 79-1482, July 1979.

[5]Berman, H. A., Anderson, J. D., Jr., and Drummond, J. P., "Supersonic Flow Over a Rearward-Facing Step with Transverse Nonreacting Hydrogen Injector," *AIAA Journal,* Vol. 21, Dec. 1983, pp. 1707–1713.

[6]Uenishi, K., and Rogers, R. C., "Three-Dimensional Computation of Mixing of Transverse Injector in a Ducted Supersonic Flow," AIAA Paper 86-1423, June 1986.

[7]Uenishi, K., Rogers, R. C., and Northam, G. B., "Three-Dimensional Computations of Transverse Hydrogen Jet Combustion in a Supersonic Airstream," AIAA Paper 87-0089, Jan. 1987.

[8]Uenishi, K., Rogers, R. C., and Northam, G. B., "Three-Dimensional Numerical Predictions of the Flow Behind a Rearward-Facing Step in a Supersonic Combustor," AIAA Paper 87-1962, June 1987.

[9]Whitehurst, R. B., "Laser-Induced Fluorescence Flow Visualization of Transverse, Gaseous Fuel Injection into a Supersonic Flow," M. S. Thesis, Univ. of Virginia, Charlottesville, VA, Jan. 1982.

[10]Fletcher, D. G., "Spatially Resolved, Nonintrusive Measurements in a Nonreacting Scramjet Combustor Using Laser-Induced Iodine Fluorescence," Ph.D. Dissertation, Univ. of Virginia, Charlottesville, VA, Jan. 1988.

[11]Torrence, M. G., "Concentration Measurements of an Injected Gas in a Supersonic Stream," NASA TN D-3860, April 1967.

[12]Weidner, J. P., and Trexler, C. A., "Preliminary Investigation of Momentum Diffusion Between Two Supersonic Airstreams in the Presence of Shock Waves," NASA TN D-4974, Jan. 1969.

[13]Orth, R. C., Schetz, J. A., and Billig, F. S., "The Interaction and Penetration of Gaseous Jets in Supersonic Flow," NASA CR-1386, July 1969.

[14]Torrence, M. G., "Effect of Injectant Molecular Weight on Mixing of a Normal Jet in a Mach 4 Airstream," NASA TN D-6061, Jan. 1971.

[15]McClinton, C. R., "The Effect of Injection Angle on the Interaction Between Sonic Secondary Jets and a Supersonic Free Stream," NASA TN D-6669, Feb. 1972.

[16]Anderson, G. Y., and Gooderum, P. B., "Exploratory Tests of Two Strut Fuel Injectors for Supersonic Combustion," NASA TN D-7581, Feb. 1974.

[17]McClinton, C. R., Torrence, M. G., Gooderum, P. B., and Young, I. G., "Nonreactive Mixing Study of a Scramjet Swept-Strut Fuel Injector," NASA TN D-8069, Dec. 1975.

[18]McDaniel, J. C., and Graves, J., Jr., "Laser-Induced Fluorescence Visualization of Transverse Gaseous Injection in a Nonreacting Supersonic Combustor," *Journal of Propulsion and Power,* Vol. 4, Nov.–Dec. 1988, pp. 591–597.

[19]Whitehurst, R. B., McDaniel, J. C., Uenishi, K., and Northam, G. B., "Experimental and Numerical Studies of Transverse Fuel-Injection Patterns in a Supersonic Combustor," AIAA Paper 87-2163, June 1987.

[20]Fletcher, D. G., and McDaniel, J. C., "Laser-Induced Iodine Fluorescence Technique for Quantitative Measurement in a Nonreacting Supersonic Combustor," *AIAA Journal,* Vol. 27, May 1989, pp. 575–580.

[21]Hersch, M., Povinelli, L. A., and Povinelli, F. P., "Optical Study of Sonic and Supersonic Jet Penetration from a Flat Plate into a Mach 2 Airstream," NASA TN D-5717, March 1970.

[22]Hartfield, R. J., Jr., Abbitt, J. D., III, and McDaniel, J. C., "Injectant Mole-Fraction Imaging in Compressible Mixing Flows Using Planar Laser-Induced Iodine Fluorescence," *Optics Letters,* Vol. 14, Aug. 1989, pp. 850–852.

[23]Mungal, M. G., and Frieler, C. E., "The Effects of Damköhler Number in a Turbulent Shear Layer," *Combustion and Flame,* Vol. 71, Jan. 1988, pp. 23–24.

[24]Tillman, T. G., Patrick, W. P., and Paterson, R. W., "Enhanced Mixing of Supersonic Jets," AIAA Paper 88-3002, July 1988.